RESULTS ON STANDARD MODEL AND FLAVOUR PHYSICS WITH THE CMS DETECTOR AT THE LHC*

Mikołaj Ćwiok

for the CMS Collaboration

University of Warsaw, Department of Physics
Hoża 69, 00-681, Warszawa, Poland

(Received April 19, 2013)

In this conference paper selected results on: quantum chromodynamics jets, electroweak vector bosons, top quark and b-hadron production are reported. The proton–proton collision data at the centre-of-mass energies of 7 TeV and 8 TeV were collected with the Compact Muon Solenoid detector at the LHC. No deviations from predictions of the Standard Model theory of particle interactions were observed after analysing data corresponding to an integrated luminosity of up to 5 fb^{-1} at each energy.

DOI:10.5506/APhysPolB.44.1395
PACS numbers: 12.38.Qk, 12.15.–y, 14.65.Ha, 13.20.He

1. Introduction

The Compact Muon Solenoid (CMS) is a general purpose detector built to study proton–proton (pp) as well as heavy ion collisions. Its tracking and calorimetry systems cover pseudorapidity[1] regions of $|\eta| < 2.4$ and $|\eta| < 5$ respectively. The silicon tracker and the calorimeters are immersed in 3.8 T uniform magnetic field created inside a superconducting solenoid. The gas-ionization muon chambers are embedded in the iron return yoke outside the solenoid. A detailed description of the CMS apparatus can be found elsewhere [1].

The CMS experiment has collected pp collision data at the centre-of-mass energy of $\sqrt{s} = 7$ TeV (2010 and 2011 runs) and $\sqrt{s} = 8$ TeV (2012 run), which correspond to an integrated luminosity of 5.5 fb^{-1} and 21.8 fb^{-1}

* Presented at the Cracow Epiphany Conference on the Physics After the First Phase of the LHC, Kraków, Poland, January 7–9, 2013.

[1] Pseudorapidity η is defined as $\eta = -\ln(\tan\frac{\theta}{2})$, where θ is the polar angle of the particle's trajectory with respect to the anticlockwise beam direction.

respectively. The instantaneous luminosity of the LHC machine was steadily growing throughout years 2010–2012 for the cost of increasing the average number of inelastic pp interactions in a single bunch crossing (pile-up)[2]. Therefore, measurements at 8 TeV required tighter on-line selection cuts and refined techniques of the off-line event reconstruction.

Experimental verification of the predictions from the Standard Model (SM) theory of electroweak and strong interactions at a TeV scale, and precise measurements of the fundamental parameters of this theory are important ingredients of the CMS physics programme. This conference paper presents several recent results on production of: hard quantum chromodynamics (QCD) jets, electroweak vector bosons, top quarks and b-hadrons. A more comprehensive and up-to-date list of CMS studies can be found at [2].

2. QCD jets

In pp collisions at LHC energies the hard scattering of incoming partons is dominated by gluon exchange [3]. The resulting quarks and gluons produced at high transverse momenta, after final state radiation and hadronisation phase, are visible as jets of particles in the detector. The total cross section is a convolution of the QCD hard scattering matrix element for two colliding partons (*i.e.* valence quarks, sea quarks or gluons) and their respective parton distribution functions (PDF) in the proton. Theoretical predictions for total cross sections are sensitive to the running strong coupling constant α_{S} and to proton PDFs, while differential cross sections allow to test: QCD radiation models, higher order matrix element calculations and resummation techniques. Nowadays perturbative QCD calculations up to next-to-leading-order (NLO) are available for inclusive jet measurements [4]. Predictions at the parton level are usually combined with parton shower Monte Carlo (MC) generators in order to compare theory with experimental data.

The rich QCD programme of the CMS experiment includes among other measurements: doubly-differential inclusive jet and dijet cross sections, ratio of 3-jet to 2-jet event rates, determination of the strong coupling constant $\alpha_{\mathrm{S}}(M_Z)$, jet invariant masses in dijet and vector boson + jet events, differential b-quark jet cross sections, as well as studies on: jet shapes, subjet multiplicities, dijet azimuthal decorrelations, forward jets and small Bjorken-x QCD, multi-parton interactions, underlying event and soft QCD.

[2] On average, the amount of pile-up interactions doubled between 2011 and 2012 runs from 9 to 21 inelastic pp interactions in a single bunch crossing.

2.1. Inclusive jet rates

Jets at the CMS are reconstructed with the Particle Flow technique [5] in which the information from several sub-detectors is combined in order to reconstruct all stable particles, which, in turn, are clustered into jets using the anti-k_{T} algorithm [6] with radius parameter $R = 0.7$.

The measured doubly-differential cross section for inclusive jet production at 7 TeV is shown in Fig. 1 [7]. Jet transverse momenta were probed up to 2 TeV for jet rapidities $|y| < 2.5$. The invariant mass spectra of two leading-p_{T} jets were also measured. The highest mass of the dijet system reached 5 TeV. All distributions were unfolded to particle level in order to correct for detector effects. The dominant experimental uncertainties are due to: jet energy scale (JES), luminosity, jet p_{T} resolution, and unfolding.

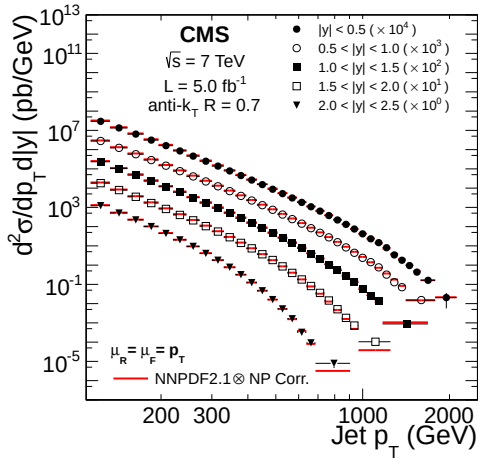

Fig. 1. Inclusive jet cross section for 5 rapidity bins for data (markers) and theory (thick lines) using the NNPDF2.1 PDF set.

The NLO theoretical predictions were computed using NLOJet++ for five proton PDF sets: NNPDF2.1, CT10, MSTW2008, HERAPDF1.5 and ABKM09. The effects of non-perturbative corrections, accounting for multi-parton interactions and hadronisation, were evaluated by comparing predictions of PYTHIA6 and HERWIG++ generators. The measured differential cross sections as a function of the leading jet p_{T} and as a function of di-jet invariant mass are compatible with NLO predictions at 10% level in all rapidity bins. For example, in Fig. 2 comparisons of the NLOJet++ and NNPDF2.1 prediction with the experimental data, and with predictions corresponding to other PDF sets are shown for central leading-p_{T} jets.

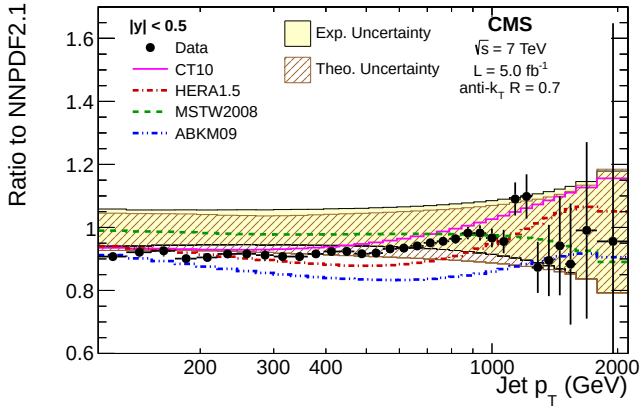

Fig. 2. Ratio of the measured inclusive jet cross section (points) to the theoretical prediction using the NNPDF2.1 PDF set for the central rapidity bin.

2.2. Ratio of inclusive trijet and dijet cross sections

The ratio of inclusive cross sections for events with three- and two-jets, R_{32}, is proportional to the strong coupling constant α_{S}. The measured differential R_{32} ratio as a function of the average p_{T} of two leading jets, $\langle p_{\mathrm{T}\,1,2}\rangle$, is depicted in Fig. 3 for 7 TeV data [8]. The NLO theory prediction combined with NNPDF2.1 proton PDF using the default value of $\alpha_{\mathrm{S}}(M_Z) = 0.119$ is in agreement with the experimental data (black solid curve in Fig. 3).

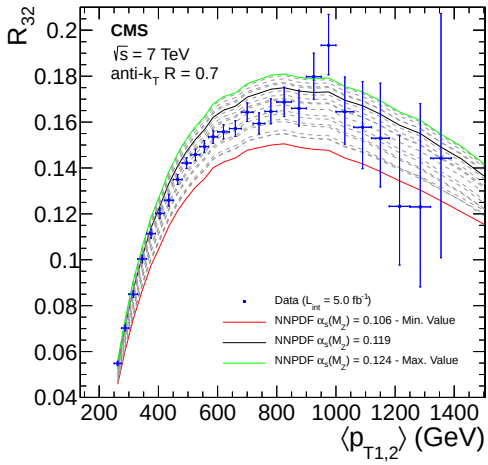

Fig. 3. Ratio of trijet to dijet event rates in data together with the NLO predictions using the NNPDF2.1 PDF set for several values of $\alpha_{\mathrm{S}}(M_Z)$.

The input value of $\alpha_S(M_Z)$ was also varied in order to get the best data and theory agreement in the most sensitive region of $\langle p_{T\,1,2} \rangle$ between 400 GeV and 1.4 TeV. The result of the fit corresponding to NNPDF2.1 proton PDF set is: $\alpha_S(M_Z) = 0.1143^{+0.0083}_{-0.0067}$. Similar results were obtained for CT10 and MSTW2008 proton PDF sets. The ABM11 PDF set was not used to extract $\alpha_S(M_Z)$ value as it failed to describe experimental data for $\langle p_{T\,1,2} \rangle < 600\,\text{GeV}$.

3. Vector bosons

The production of electroweak vector bosons $W^{\pm}$, Z^0 and γ at the LHC occurs primarily via Drell–Yan process [3]. In particular, final states with electrons and muons have clean experimental signatures and are well established theoretically. Studying single boson, diboson and vector boson associated with jets processes, besides testing of the SM at a TeV scale, allows one to: calibrate and align detector components (*e.g.* jet energy scale, source of prompt muons), constrain proton PDFs (*e.g.* probe Bjorken-x region between 10^{-3} and 0.1, probe contribution of sea quarks).

Many analyses, such as: top quark measurements, Higgs boson searches or beyond SM searches, rely on the accurate theoretical modelling of the SM backgrounds involving vector bosons. Several tools are available nowadays to predict vector boson + jets rates at hadron colliders, including: leading-order (LO) matrix element with parton shower matching (*e.g.* ALPGEN+HERWIG [9], MADGRAPH+PYTHIA [10], SHERPA [11]), fixed order NLO (*e.g.* BLACKHAT+SHERPA [12], ROCKET+MCFM [13, 14]), fixed order NLO with parton shower matching (*e.g.* POWHEG+PYTHIA [15], MC@NLO [16], MENLOPS [17], MEPS@NLO [18]), approximate next-to-next-leading-order (NNLO) (*e.g.* LOOPSIM+MCFM [19]), and all order resummation (*e.g.* HEJ [20]).

The CMS measurements of vector boson production in pp collisions include: total cross sections for inclusive W and Z production ($W \to \ell\nu$, $Z \to \ell\ell$, $Z \to 4\ell$), differential observables in Drell–Yan Z production (forward–backward asymmetry A_{FB}, extraction of the weak mixing angle θ_W, rapidity and p_T spectra of Z bosons), differential lepton charge asymmetry A_C in W events, W boson polarisation in $W \to \ell\nu$ events, differential cross sections for W+jets and Z+jets, total cross sections for vector boson associated with heavy flavour jets ($W + c$, $Z + b$, $Z + b\bar{b}$), total cross sections for diboson production (WW, ZZ, WZ, $W\gamma$, $Z\gamma$), and differential cross section for isolated diphoton production. In addition, limits on anomalous triple gauge couplings for several extensions of the SM were also set. The measured and predicted cross sections for several inclusive vector boson production modes at 7 TeV and 8 TeV are summarized in Fig. 4.

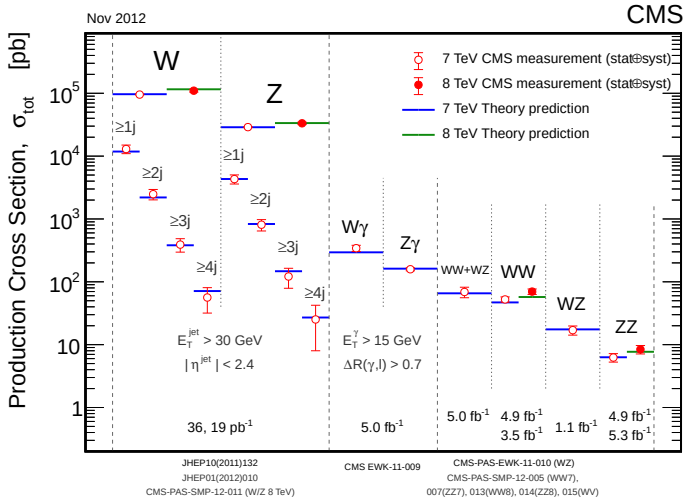

Fig. 4. Measured and predicted total cross sections for several vector boson production modes in pp collisions at 7 TeV and 8 TeV.

3.1. Determination of $\sin^2\theta_{\mathrm{W}}$

The effective weak mixing angle, $\theta_{\mathrm{W}}^{\mathrm{eff}}$, can be determined from Drell–Yan production of the neutral Z^0 and γ^* bosons decaying into a pair of charged leptons. In the frame of annihilating $q\bar{q}$ pair a distribution of the θ^* angle between the incoming quark q and the outgoing lepton ℓ^- is asymmetric. This asymmetry is also visible in symmetric pp collisions because direction of a valence quark is more likely to be along the dilepton boost direction.

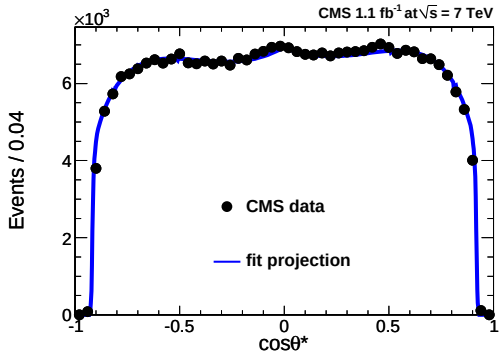

Fig. 5. Measured (points) and fitted (solid line) distribution of $\cos\theta^*$ in Drell–Yan $q\bar{q} \to Z/\gamma^* \to \mu^+\mu^-$ events.

The CMS collaboration measured the forward–backward asymmetry in $Z \to \mu^+\mu^-$ events in pp collisions at 7 TeV using dataset corresponding to 1.1 fb^{-1} [21]. Shapes of the observed kinematic distributions of: dilepton rapidity, dilepton invariant mass and decay angle θ^* were compared with theoretical predictions using different input values of $\sin^2\theta_{\mathrm{W}}^{\mathrm{eff}}$. One of such distributions is shown in Fig. 5. A simultaneous fit to all three distributions yielded value of $\sin^2\theta_{\mathrm{W}}^{\mathrm{eff}} = 0.2287 \pm 0.0020\,(\mathrm{stat.}) \pm 0.0025\,(\mathrm{syst.})$. The main sources of systematics were due to: proton PDFs, final state radiation models, effects beyond the LO in QCD and alignment of the tracker.

The CMS result has a precision of 1% after analysing only part of the available experimental data at 7 TeV. Although this precision is not as good as for experiments at LEP (0.1%) or at Tevatron (0.5%), it is already comparable with results published by NuTeV and H1 experiments (1–2%).

3.2. Z+jets measurements

Events where a Z boson is produced in association with jets in pp collisions are useful for testing predictions of perturbative QCD calculations at the highest accessible energies and for a broad range of kinematic configurations. Such predictions include: LO multiparton matrix-elements with up to 4 hard partons in the final state (*e.g.* MADGRAPH+PYTHIA, SHERPA) and NLO simulations of Z boson with 1-jet events (*e.g.* POWHEG+PYTHIA).

The jet multiplicities, event shapes and azimuthal correlations in $Z(\to \ell^+\ell^-)+\mathrm{jets}$ events were measured with the CMS detector at 7 TeV using 5.0 fb^{-1} of data [22]. Events were required to have: at least one jet,

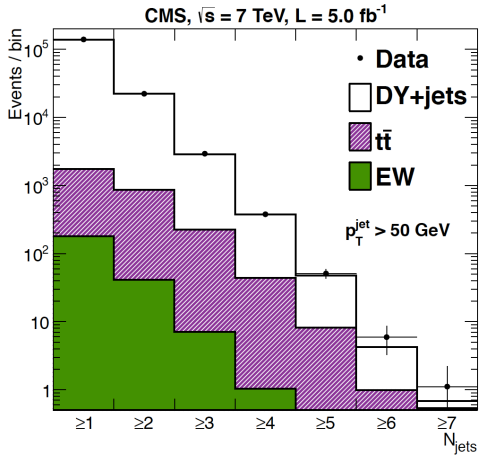

Fig. 6. Inclusive jet multiplicity in data and MC of the dimuon candidates within a window of 20 GeV around M_Z.

two opposite-sign leptons with high p_{T} and the dilepton invariant mass consistent with a Z boson candidate. All data distributions were corrected for detector resolution effects and unfolded to the particle level.

The results on jet multiplicities in $Z \to \mu^+\mu^-$ events with $p_{\mathrm{T}}^Z > 50\,\mathrm{GeV}$ are presented in Fig. 6. Predictions from the MADGRAPH generator are also superimposed in the figure. Event shapes were studied for two kinematic regions of Z bosons: all p_{T}^Z and $p_{\mathrm{T}}^Z > 150\,\mathrm{GeV}$. The following observables in the azimuthal plane were exploited: $\Delta\phi(Z, \mathrm{jet}_i)$, $\Delta\phi(\mathrm{jet}_i, \mathrm{jet}_j)$ and transverse thrust τ_{T}, where jet_i denotes the ith leading-p_{T} jet in the event. For example, the angular correlations between the Z boson and the leading jet are shown in Fig. 7 for events with different jet multiplicities. Overall, the measured observables are in good agreement with those simulated by MADGRAPH+PYTHIA and SHERPA generators for two kinematic regions studied.

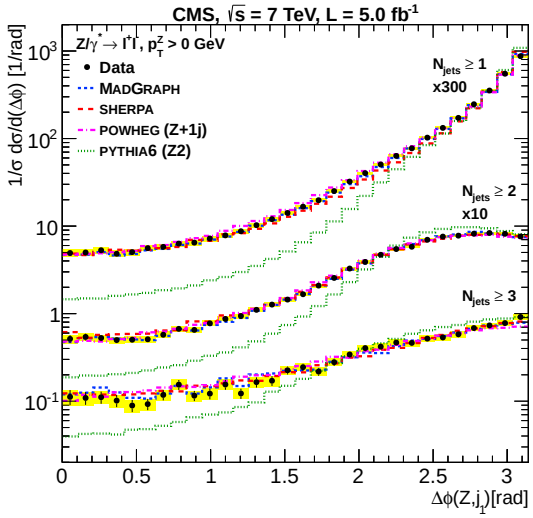

Fig. 7. Distribution of the dijet invariant mass spectrum in data (points) and MC simulation (solid histogram) after subtraction of all components except the electroweak $WW + WZ$ processes.

3.3. Diboson WW/WZ measurements

The diboson WW and WZ production in pp collisions proceeds primarily via t-channel and s-channel quark annihilation. The former process has a three-boson vertex (WWZ or $WW\gamma$).

The CMS collaboration measured the inclusive $WW + WZ$ diboson production cross section at 7 TeV using $W + 2$ jets final states ($e\nu jj$ and $\mu\nu jj$) from data corresponding to 5.0 fb^{-1} [23]. The event yields for the signal were determined from the distribution of the invariant mass, m_{jj}, of two

non-b jets in the event. Contributions due to other known SM processes, such as: W+jets, $t\bar{t}$, single top, QCD, and Z+jets, were estimated using an unbinned maximum-likelihood fit over the mass range between 40 GeV and 150 GeV. The shapes of the background distributions were simulated with MADGRAPH, POWHEG and PYTHIA generators.

The m_{jj} distribution, after subtraction of all components except the electroweak $WW + WZ$ processes, is shown in Fig. 8 for combined electron and muon channels. The measured sum of the inclusive WW and WZ cross sections is: $\sigma(pp \to WW + WZ) = 68.9 \pm 8.7\,(\text{stat.}) \pm 9.7\,(\text{syst.}) \pm 1.5\,(\text{lum.})$ pb. The dominant systematic uncertainties are due to: theory uncertainty on acceptance, luminosity determination, lepton reconstruction and selection efficiencies, trigger efficiency, jet energy scale, missing transverse energy resolution, and fit uncertainty. The result agrees with the NLO SM prediction of 65.6 ± 2.2 pb. In addition, no evidence of anomalous triple gauge couplings was found from the tails of the measured dijet p_{T} distributions.

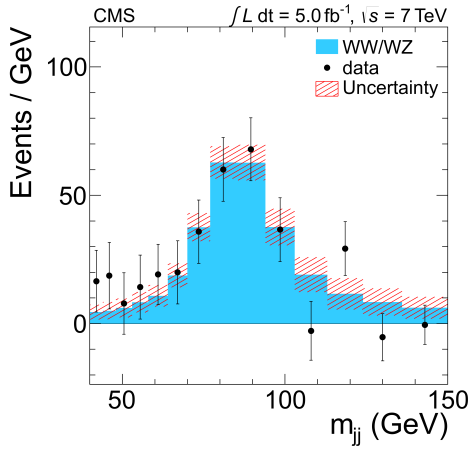

Fig. 8. Azimuthal correlations between the Z boson and the leading-p_{T} jet in data and MC simulations. Electron and muon channels are combined.

4. Top quarks

The LHC machine has delivered about 1×10^6 (5×10^6) top quark pairs during 2011 (2012) run to each of the ATLAS and CMS experiments. This top quark factory allows to test many aspects of the SM such as: top production modes, top quark properties and decays.

Studies of top quark production modes include: cross sections for $t\bar{t}$ pairs produced via QCD processes with various final states, cross sections for the electroweak single top production, asymmetries and spin correlations in $t\bar{t}$ production, searches for possible new states decaying into top quarks.

The top quark mass, m_t, is a fundamental parameter of the SM and many theoretical predictions depend on this value. Other properties of interest are: mass difference between t and $\bar{t}$ quarks, width and lifetime, electric charge, and probability of boson radiation.

Top quark decays proceed almost exclusively through $t \to Wb$, allowing to measure helicity of W bosons. Top decays are also important for searches beyond the SM, such as: anomalous Wtb couplings, charged Higgs boson production in top decays, flavour-changing neutral current decays: $t \to qZ/q\gamma/qg$.

4.1. $t\bar{t}$ pair production

At energies exploited by the LHC, about 80% of top quark pairs are created by gg fusion [3]. The branching fractions of $t\bar{t}$ final states categorized according to W boson decays are the following:

— 46% from all hadronic mode (*i.e.* 4 light jets and 2 b-jets),

— 45% from lepton + jets mode (*i.e.* $e/\mu/\tau$, 2 b-jets and missing E_{T}),

— 9% from dileptonic mode (*i.e.* $ee/\mu\mu/e\mu/e\tau/\mu\tau$, 2 b-jets and missing E_{T}).

The CMS collaboration has published several results on $t\bar{t}$ production cross section, $\sigma_{t\bar{t}}$, measured from different final states at 7 TeV (8 TeV) using data corresponding to an integrated luminosity of up to 3.9 fb^{-1} (2.8 fb^{-1}) [24, 25]. These measurements, together with the available NNLO predictions from the SM, are summarized in Figs. 9 and 10 for 2011 and 2012 runs, respectively. The following combinations of $\sigma_{t\bar{t}}$ measurements are available to date:

— CMS data corresponding to $0.8 - 1.1$ fb^{-1} per channel:
$\sigma_{t\bar{t}}(\sqrt{s} = 7\,\mathrm{TeV}) = 165.8 \pm 2.2\,(\mathrm{stat.}) \pm 10.6\,(\mathrm{syst.}) \pm 7.8\,(\mathrm{lum.})$ pb [26],

— CMS data corresponding to $2.4 - 2.8$ fb^{-1} per channel:
$\sigma_{t\bar{t}}(\sqrt{s} = 8\,\mathrm{TeV}) = 227 \pm 3\,(\mathrm{stat.}) \pm 11\,(\mathrm{syst.}) \pm 10\,(\mathrm{lum.})$ pb [25],

— ATLAS and CMS data corresponding to up to 1.1 fb^{-1} per experiment:
$\sigma_{t\bar{t}}(\sqrt{s} = 7\,\mathrm{TeV}) = 173.3 \pm 2.3\,(\mathrm{stat.}) \pm 9.8\,(\mathrm{syst.})$ pb [27].

All results agree with the approximate NNLO perturbative QCD calculations. Cross sections derived from dilepton final states have the smallest experimental errors which are comparable to theoretical uncertainties.

The SM predicts charge asymmetry in $t\bar{t}$ production arising from interference between QCD, QED and weak diagrams. In symmetric proton–proton collisions at the LHC only $t\bar{t}$ pairs created by annihilation of valence quarks

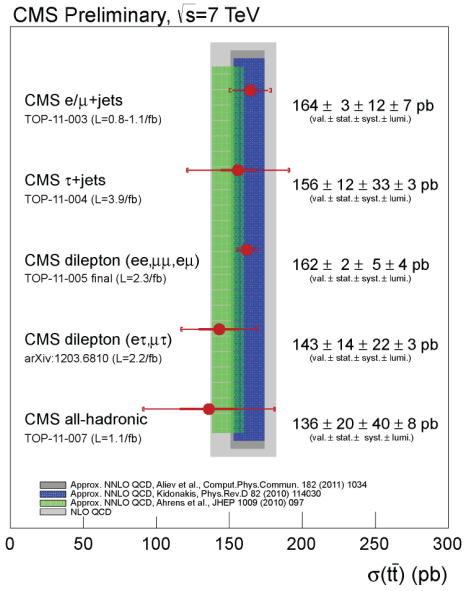

Fig. 9. Measured cross section for $t\bar{t}$ production in different channels at 7 TeV. The data are compared to the approximate NNLO calculations.

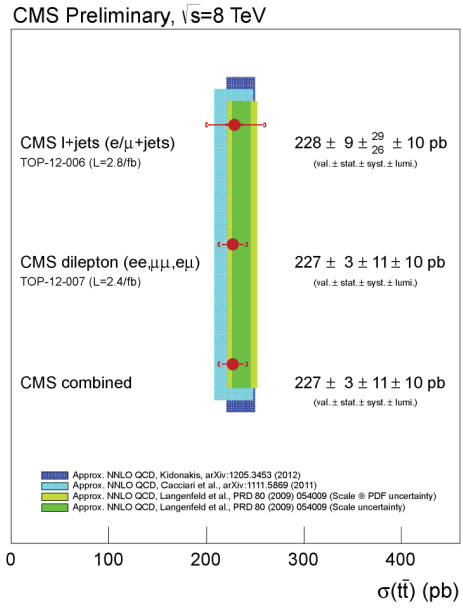

Fig. 10. Measured cross section for $t\bar{t}$ production in different channels at 8 TeV. The data are compared to the approximate NNLO calculations.

and sea anti-quarks contribute to this effect. The rapidity distribution of t quarks is slightly broader than that of $\bar{t}$ quarks. This results in a non-zero charge asymmetry defined as $A_{\mathrm{C}}^{y} = \frac{N(\Delta_y>0)-N(\Delta_y<0)}{N(\Delta_y>0)+N(\Delta_y<0)}$, where N denotes the number of events in a given category and $\Delta_y = |y_t| - |y_{\bar{t}}|$. The asymmetries measured with the CMS detector at 7 TeV are the following [28]:

— $A_{\mathrm{C}}^{y} = 0.050 \pm 0.043\,(\mathrm{stat.})^{+0.010}_{-0.039}\,(\mathrm{syst.})$ from the dilepton channel (the distribution of Δ_y is shown in Fig. 11),

— $A_{\mathrm{C}}^{y} = 0.004 \pm 0.010\,(\mathrm{stat.}) \pm 0.012\,(\mathrm{syst.})$ from the ℓ+jets channel.

Both results agree with the SM prediction of $A_{\mathrm{C}}^{y} = 0.0115 \pm 0.0006$, although present experimental uncertainties are still large.

The CMS Collaboration also performed the first measurement of the cross section ratio $\sigma(pp \to t\bar{t}\,b\bar{b})/\sigma(pp \to t\bar{t}\,jj)$, where jj ($b\bar{b}$) denote two jets (two b-jets) present in addition to two b-quarks from decays of top quarks. The production of a top quark pair in association with a $b\bar{b}$ pair is predicted by higher order QCD. It constitutes the irreducible background for the associated Higgs boson production with a $t\bar{t}$ pair. The measured cross section ratio at 7 TeV using dataset corresponding to an integrated luminosity of 5.0 fb^{-1} is: $(3.6 \pm 1.1\,(\mathrm{stat.}) \pm 0.9\,(\mathrm{syst.})) \times 10^{-2}$ [29]. This result is compatible with MC predictions of MADGRAPH (1.2×10^{-2}) and POWHEG (1.3×10^{-2}) generators.

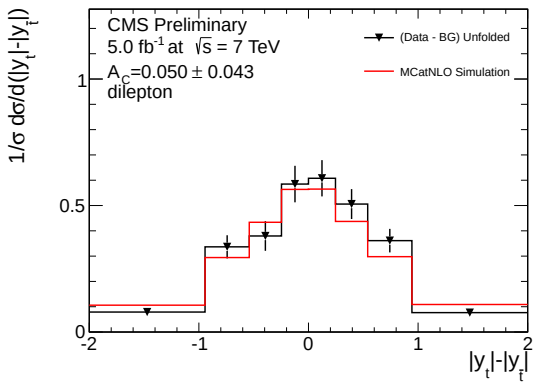

Fig. 11. Measured and predicted distribution of the difference between absolute rapidity of t and $\bar{t}$ quarks in dilepton channels.

Another important test of the validity of the SM is production of top quark pairs in association with vector bosons (W or Z). The CMS collaboration provided 4.6σ evidence for such $t\bar{t}V$ production by studying $t\bar{t}$ pairs having the same-sign dileptonic or trileptonic final states. The measured

sum of $t\bar{t}W$ and $t\bar{t}Z$ cross sections at 7 TeV and corresponding to an integrated luminosity of 4.98 fb^{-1} is: $\sigma_{t\bar{t}V} = 0.51^{+0.15}_{-0.13}\,(\text{stat.})^{+0.05}_{-0.04}\,(\text{syst.})$ pb [30]. It is compatible with the NLO prediction of 0.308 pb.

4.2. Top quark mass

The CMS Collaboration uses several techniques to measure m_t in different $t\bar{t}$ final states:

— Jet energy scale *in situ* calibration — uses invariant mass of two light jets from W boson decay to constrain the JES.

— Templates method — compares data with MC simulation for observables sensitive to m_t.

— Analytical matrix element weighting — constructs event probability density that the event with certain input m_t would lead to variables observed in the detector.

— Ideogram method — calculates event-by-event two-dimensional likelihood as a function of m_t and JES, and considers all permutations of jet assignments to top quark decays.

— Kinematic endpoints method — explores variables suited to analyse events with symmetric three-body decay.

— Indirect measurement from the $t\bar{t}$ cross section — parametrises dependence of the measured and predicted $\sigma_{t\bar{t}}$ on m_t.

The main sources of systematic uncertainties are due to: jet energy scales for light-jets and b-jets, lepton energy scale, MC simulation (*e.g.* parton-level modelling, initial and final state radiation, factorisation and renormalisation scales, matrix-element to parton-shower matching, proton PDFs, underlying event, background), jet energy resolution, b-tagging, missing E_{T} scale, colour reconnection, pile-up, and trigger.

The results on m_t corresponding to 7 TeV data recorded in 2010 and 2011 using different $t\bar{t}$ final states are summarized in Fig. 12. The combination of these results yields: $m_t = 173.4 \pm 0.4\,(\text{stat.}) \pm 0.9\,(\text{syst.})$ GeV [31]. The current LHC combination of m_t measurements uses only part of the data collected in 2011 (*i.e.* up to 2.0 fb^{-1} from ATLAS and up to 4.9 fb^{-1} from CMS) which results in: $m_t = 173.3 \pm 0.5\,(\text{stat.}) \pm 1.3\,(\text{syst.})$ GeV [32]. The precision on m_t from a single experiment at the LHC is already comparable with the combined result of CDF and D0 experiments at the Tevatron.

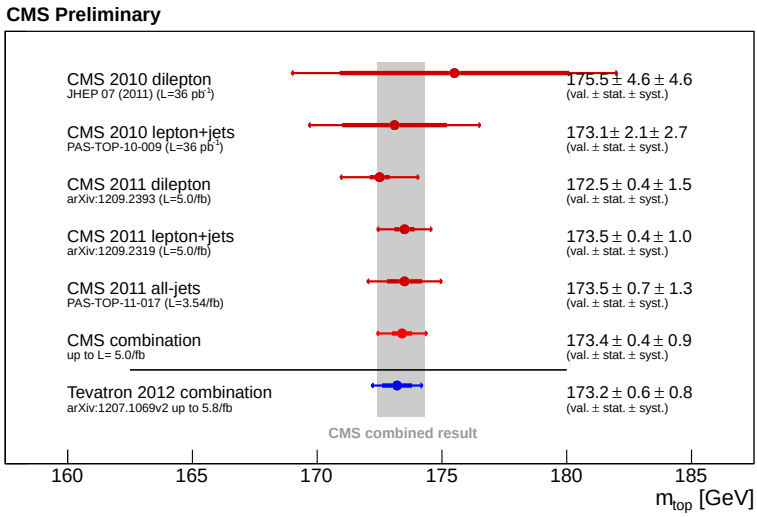

Fig. 12. Summary of the top quark mass measurements at 7 TeV in different channels.

4.3. Single top quark production

The electroweak production of single top quarks in pp collisions can proceed via three processes: t-channel exchange of a virtual W boson, associated production of a top quark and a W boson, and s-channel production and decay of a virtual W boson. At LHC energies the s-channel has the smallest cross section between these production modes[3] and is yet to be observed by CMS and ATLAS experiments.

The CMS collaboration studied the t-channel production mode at 7 TeV and at 8 TeV using datasets corresponding to an integrated luminosity of 1.16 fb^{-1} and 5.0 fb^{-1} respectively. Events were required to have: one isolated charged lepton (e or μ) and a missing E_{T} (from the leptonic W boson decay), and one central b-jet (from the top-quark decay). Two methods were exploited to extract the signal: the distributions of the pseudorapidity of the jet recoiling against the top quark, and multivariate analyses based on Boosted Decision Trees (BDT) or Neural Networks. The main sources of systematic uncertainties are due to: MC modelling of W+jets events, b-tagging and theoretical predictions for $t\bar{t}$ and other single top channels. The measured cross sections for the single top production via the t-channel are the following:

[3] Predicted cross sections for the s-channel are about 5 pb and 6 pb at $\sqrt{s} = 7$ TeV and 8 TeV respectively. The single top production via the s-channel has been already observed in $p\bar{p}$ collisions at $\sqrt{s} = 1.96$ TeV at the Tevatron.

— $\sigma_{t\text{-ch.}}(\sqrt{s} = 7\,\text{TeV}) = 67.2 \pm 3.7\,(\text{stat.}) \pm 3.0\,(\text{syst.}) \pm 3.5\,(\text{theor.}) \pm 1.5\,(\text{lum.})$ pb [33],

— $\sigma_{t\text{-ch.}}(\sqrt{s} = 8\,\text{TeV}) = 80.1 \pm 5.7\,(\text{stat.}) \pm 11.0\,(\text{syst.}) \pm 4.0\,(\text{lum.})$ pb [34].

From Fig. 13 one can see that all experimental data are consistent with the approximate NLO and next-to-next-leading-logarithm (NNLL) perturbative QCD calculations. In addition, the absolute value of the CKM element $|V_{tb}|$ was determined from 7 TeV data to be: $0.92 < |V_{tb}| \leq 1$ at the 95% confidence level provided that there are no anomalous Wtb couplings.

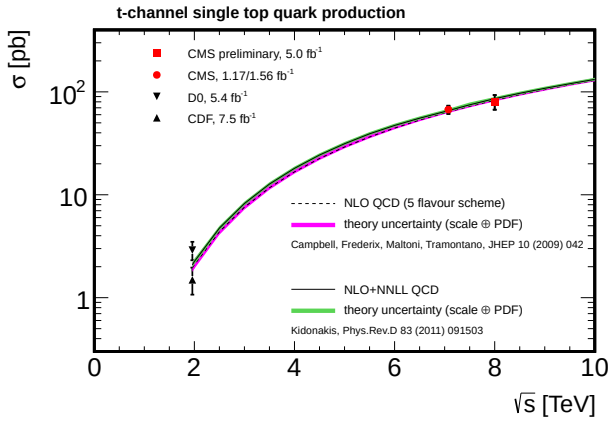

Fig. 13. Measured and predicted cross sections for single top production via the t-channel at 7 TeV and 8 TeV. Results from the Tevatron $p\bar{p}$ collider are also superimposed.

The measurement of the cross section for associated $t+W$ production was performed by CMS using 7 TeV data with final states having: two isolated leptons with opposite charge, a jet from the fragmentation of a b-quark, and a large missing E_{T} from the two neutrinos. Two methods were used for separating signal events from the background: the cut-based analysis and the multivariate one based on BDTs. In Fig. 14 the distribution of BDT discriminant variable is shown along with the expected background due to $t\bar{t}$ and Z/γ^*+jets production. The measured cross sections corresponding to an integrated luminosity of 4.9 fb^{-1} are the following [35]:

— $\sigma_{t+W} = 16^{+5}_{-6}$ pb from BDT method (significance of 4.0σ),

— $\sigma_{t+W} = 15 \pm 5$ pb from event cutting method (significance of 3.5σ).

The dominant systematic uncertainties are from JES and theoretical predictions on $t\bar{t}$ and associated $t + W$ production. The data are consistent with the SM approximate NNLO prediction of 15.6 ± 1.3 pb.

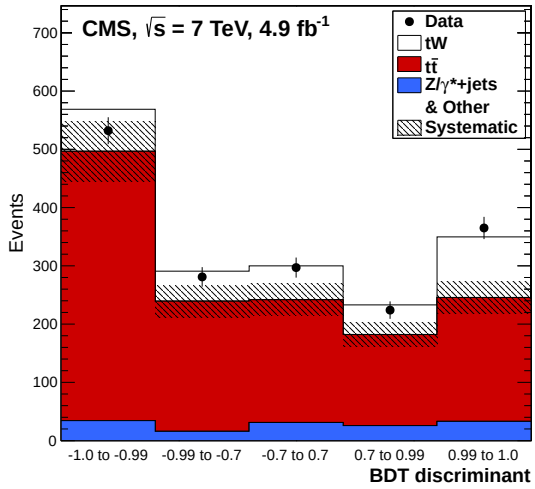

Fig. 14. Distribution of the BDT discriminant in the single top signal region ($1j1t$) in data and simulation at 7 TeV.

5. Heavy flavours

The proton–proton collisions at high centre-of-mass energies are well suited for studying heavy quarkonia as well as charmed- and bottom-hadron production over a wide kinematic range. Some topics of particular interest are: J/ψ and Υ differential production cross sections and polarizations, heavy flavour spectroscopy for verification of the lattice QCD and non-relativistic QCD techniques, rare B and D meson decays for testing CP violation and looking for signs of New Physics.

The CMS detector and reconstruction algorithms are optimized for heavy flavour physics in many ways, such as: good track p_{T} and vertex position resolutions in the tracker, good dimuon mass resolution, high muon reconstruction efficiency and purity and dedicated b-hadron and quarkonium triggers from dimuons.

5.1. Discovery of Ξ_b^{*0} baryon

The SM predicts existence of the excited b-baryon Ξ_b^{*0} consisting of a usb quark triplet with $J^{\mathrm{P}} = \frac{3}{2}^{+}$. A search for this state has been performed in CMS using 7 TeV data corresponding to an integrated luminosity

of 5.3 fb^{-1} [36]. The following chain of decays was exploited: $\Xi_b^{*0} \to \Xi_b^- \pi^+$, $\Xi_b^- \to J/\psi\,\Xi^-$, $J/\psi \to \mu^+\mu^-$, $\Xi^- \to \Lambda^0\,\pi^-$ and $\Lambda^0 \to \pi^+\pi^-$, and their respective charge conjugates. Events were required to have three displaced vertices in addition to the primary one. In Fig. 15 a peak is clearly visible in distribution of the difference between the mass of the $\Xi_b^-\,\pi^+$ system and the sum of the masses of Ξ_b^- and π^+. The signal is observed with a significance of $5.7\,\sigma$ and the fitted mass and width of this new state are: $M(\Xi_b^{*0}) = 5945.0 \pm 0.7\,(\text{stat.}) \pm 0.3\,(\text{syst.}) \pm 2.7\,(\text{PDG})\,\text{MeV}$ and $\Gamma(\Xi_b^{*0}) = 2.1 \pm 1.7\,(\text{stat.})\,\text{MeV}$. These data are compatible with predictions of the lattice QCD calculations.

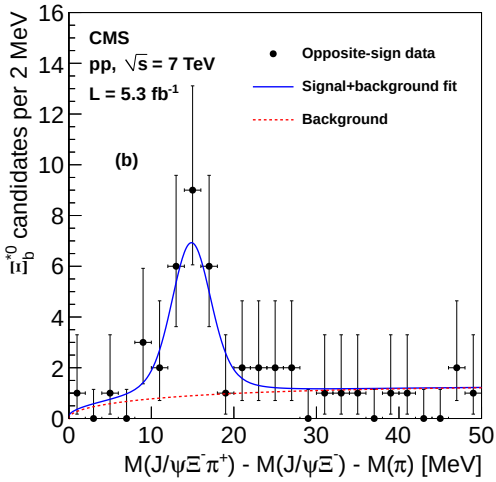

Fig. 15. Distribution of candidate events for new Ξ_b^{*0} baryon state produced in pp collisions at 7 TeV.

5.2. b-hadron production

The CMS experiment performed measurements of the total and differential cross sections for several b-hadrons such as: B^+, B^0, B_s^0 and Λ_b [37]. The total cross sections measured at 7 TeV using up to 1.9 fb^{-1} of collision data are presented in Fig. 16. The experimental data are in agreement with the NLO SM predictions calculated with the MC@NLO+POWHEG generator, although all predictions tend to be slightly lower than data. The measured distributions of the b-hadron transverse momenta are shown in Fig. 17. The observed p_{T} distribution for the Λ_b baryon is falling more steeply than distributions for B mesons.

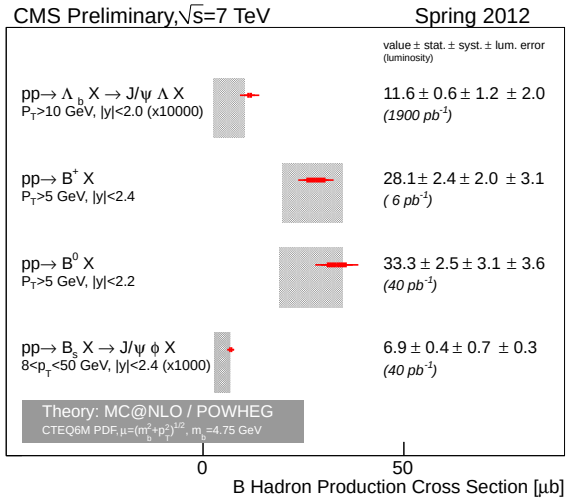

Fig. 16. Summary of b-hadron cross section measurements performed by CMS with 7 TeV pp collisions.

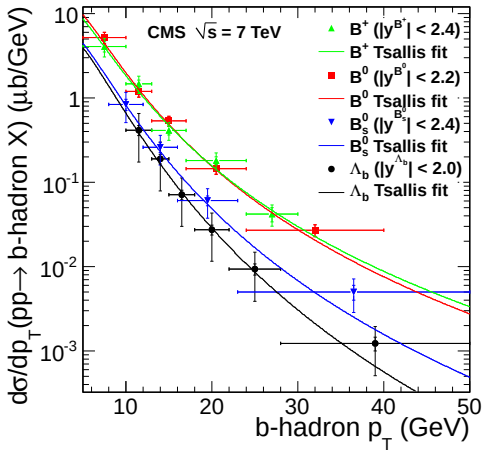

Fig. 17. Comparison of b-hadron production rates as a function of hadron transverse momentum in pp collisions at 7 TeV.

5.3. Rare B meson decays

The decays: $B^0 \to \mu^+\mu^-$ and $B_s^0 \to \mu^+\mu^-$ are highly suppressed in the SM with the following predicted branching fractions: $\mathcal{B}(B^0 \to \mu^+\mu^-) = (1.07 \pm 0.10) \times 10^{-10}$ and $\mathcal{B}(B_s^0 \to \mu^+\mu^-) = (3.23 \pm 0.27) \times 10^{-9}$. They can only proceed via high-order Z-penguin and box diagrams and, therefore, are sensitive to the extended Higgs boson sectors beyond the SM.

A search for these rare B meson decays was done by the CMS collaboration using pp collision data collected at 7 TeV and corresponding to an integrated luminosity of 5 fb^{-1} [38]. A blind analysis was performed in dimuon mass regions around the B_s^0 and B^0 masses. The number of background events due to B decays was taken from the MC simulation and due to the combinatorial background from sidebands of the dimuon mass window. The dimuon invariant mass distribution measured in the barrel region of the CMS detector is shown in Fig. 18. The number of observed events is consistent with the SM expectation for signal plus background. The resulting upper limits at 95% C.L. are: $\mathcal{B}(B^0 \to \mu^+\mu^-) < 1.8 \times 10^{-9}$ and $\mathcal{B}(B_s^0 \to \mu^+\mu^-) < 7.7 \times 10^{-9}$. Recently, the LHCb collaboration presented a 3.5σ evidence for $B_s^0 \to \mu^+\mu^-$ signal [39]. It would be interesting to see if ATLAS and CMS experiments will be able to independently confirm this observation after analysing full statistics collected at 7 TeV and 8 TeV.

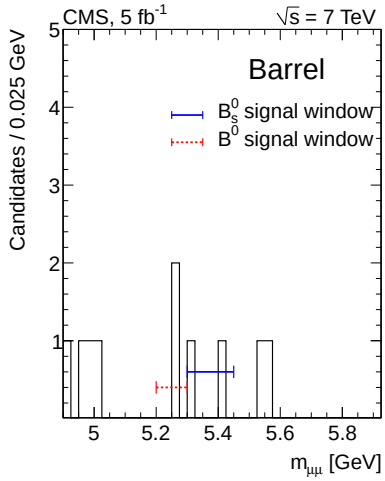

Fig. 18. Event yields for $B_s^0 \to \mu^+\mu^-$ and $B_d^0 \to \mu^+\mu^-$ decays in pp collisions at 7 TeV. Horizontal lines indicate signal windows.

6. Summary and outlooks

Selected results of the Standard Model physics programme carried out by the CMS experiment have been presented:

— hard QCD jets — probed up to transverse momenta of 2 TeV and dijet masses of 5 TeV,

— vector bosons — measured the effective weak mixing angle in Drell–Yan events, tested perturbative QCD calculations at higher orders, set new limits on anomalous triple gauge couplings,

— top quarks — verified perturbative QCD predictions for top quark pair production, m_t measured with precision comparable to Tevatron combination, observed two out of three possible single top production modes,

— heavy flavour sector — new spectroscopy measurements, studied exclusive b-hadron production, improved limits on rare B meson decays.

The SM analyses using 7 TeV data have been published or are being finalized, and several preliminary results at 8 TeV are already available. Many differential and doubly-differential observables have been measured thanks to the abundance of data. All observables are in agreement with the NLO or NNLO predictions from the Standard Model.

The first phase of running of the LHC machine has just ended. The pp collisions will be resumed in 2015 at the design centre-of-mass energy of 13–14 TeV. By that time, more SM precision measurements profiting from the full statistics collected at 7 TeV and 8 TeV should be available, along with combined results from different channels and between different LHC experiments.

REFERENCES

[1] CMS Collaboration, *JINST* **3**, S08004 (2008).

[2] CMS experiment public results: `http://twiki.cern.ch/twiki/bin/view/CMSPublic/PhysicsResults`

[3] J.M. Campbell, J.W. Huston, W.J. Stirling, *Rep. Prog. Phys.* **70**, 89 (2007).

[4] Z. Nagy, *Phys. Rev.* **D68**, 094002 (2003); W.T. Giele, E.W.N. Glover, D.A. Kosower, *Nucl. Phys.* **B403**, 633 (1993).

[5] CMS Collaboration, CMS-PAS-PFT-09-001, 2009.

[6] M. Cacciari, G.P. Salam, G. Soyez, *J. High Energy Phys.* **04**, 063 (2008).

[7] CMS Collaboration, `arXiv:1212.6660 [hep-ex]`, submitted to *Phys. Rev.* **D**.

[8] CMS Collaboration, CMS-PAS-QCD-11-003, 2011.

[9] M.L. Mangano *et al.*, *J. High Energy Phys.* **07**, 001 (2003).

[10] J. Alwall *et al.*, *J. High Energy Phys.* **06**, 128 (2011).

[11] T. Gleisberg *et al.*, *J. High Energy Phys.* **02**, 007 (2009).

[12] C.F. Berger *et al.*, *Phys. Rev.* **D78**, 036003 (2008).

[13] R.K. Ellis *et al.*, *J. High Energy Phys.* **01**, 012 (2009).

[14] J.M. Campbell, R.K. Ellis, *Nucl. Phys. B Proc. Suppl.* **205–206**, 10 (2010).

[15] S. Frixione, P. Nason, C. Oleari, *J. High Energy Phys.* **11**, 070 (2007).

[16] S. Frixione, B.R. Webber, *J. High Energy Phys.* **06**, 029 (2002).

[17] S. Höche *et al.*, *J. High Energy Phys.* **08**, 123 (2011).

[18] S. Höche *et al.*, `arXiv:1207.5030 [hep-ph]`.

[19] M. Rubin, G.P. Salam, S. Sapeta, *J. High Energy Phys.* **09**, 084 (2010).

[20] J.R. Andersen, T. Hapola, J.M. Smillie, *J. High Energy Phys.* **09**, 047 (2012).

[21] CMS Collaboration, *Phys. Rev.* **D84**, 112002 (2011).

[22] CMS Collaboration, `arXiv:1301.1646 [hep-ex]`, submitted to *Phys. Lett.* **B**.

[23] CMS Collaboration, *Eur. Phys. J.* **C73**, 2283 (2013).

[24] CMS Collaboration, *Phys. Lett.* **B720**, 83 (2013); `arXiv:1301.5755 [hep-ex]`; *J. High Energy Phys.* **11**, 067 (2012); `arXiv:1302.0508 [hep-ex]`; *Phys. Rev.* **D85**, 112007 (2012).

[25] CMS Collaboration, CMS-PAS-TOP-12-006; CMS-PAS-TOP-12-007, 2012.

[26] CMS Collaboration, CMS-PAS-TOP-11-024, 2012.

[27] ATLAS, CMS Collaborations, CMS-PAS-TOP-12-003, ATLAS-CONF-2012-134, 2012.

[28] CMS Collaboration, *Phys. Lett.* **B717**, 129 (2012); CMS-PAS-TOP-12-010, 2012.

[29] CMS Collaboration, CMS-PAS-TOP-12-024, 2012.

[30] CMS Collaboration, `arXiv:1303.3239 [hep-ex]`, submitted to *Phys. Rev. Lett.*

[31] CMS Collaboration, CMS-PAS-TOP-11-018, 2012.

[32] ATLAS, CMS Collaborations, CMS-PAS-TOP-12-001, ATLAS-CONF-2012-095, 2012.

[33] CMS Collaboration, *J. High Energy Phys.* **12**, 035 (2012).

[34] CMS Collaboration, CMS-PAS-TOP-12-011, 2012.

[35] CMS Collaboration, *Phys. Rev. Lett.* **110**, 022003 (2013).

[36] CMS Collaboration, *Phys. Rev. Lett.* **108**, 252002 (2012).

[37] CMS Collaboration, *Phys. Lett.* **B714**, 136 (2012); *Phys. Rev. Lett.* **106**, 112001 (2011); *Phys. Rev. Lett.* **106**, 252001 (2011); *Phys. Rev.* **D84**, 052008 (2011).

[38] CMS Collaboration, *J. High Energy Phys.* **04**, 033 (2012); CMS-PAS-BPH-12-009.

[39] LHCb Collaboration, *Phys. Rev. Lett.* **110**, 021801 (2013).